



Relation between leaf area index and NDVI for subarctic deciduous vegetation

W. G. Rees , E. I. Golubeva , O. V. Tutubalina , M. V. Zimin & A. A. Derkacheva

To cite this article: W. G. Rees , E. I. Golubeva , O. V. Tutubalina , M. V. Zimin & A. A. Derkacheva (2020) Relation between leaf area index and NDVI for subarctic deciduous vegetation, International Journal of Remote Sensing, 41:22, 8573-8589, DOI: [10.1080/01431161.2020.1782505](https://doi.org/10.1080/01431161.2020.1782505)

To link to this article: <https://doi.org/10.1080/01431161.2020.1782505>



Published online: 04 Sep 2020.



Submit your article to this journal [↗](#)



Article views: 75








View related articles [↗](#)



View Crossmark data [↗](#)



Relation between leaf area index and NDVI for subarctic deciduous vegetation

W. G. Rees ^a, E. I. Golubeva ^{b,#}, O. V. Tutubalina ^b, M. V. Zimin ^{b,d}
and A. A. Derkacheva ^{b*}

^aScott Polar Research Institute, University of Cambridge, Cambridge, UK; ^bFaculty of Geography, M.V. Lomonosov Moscow State University, Moscow, Russia; [#]Immanuel Kant Baltic Federal University, Kaliningrad, Russia; ^dR&D Centre ScanEx, Moscow, Russia

ABSTRACT


We consider the relationship between leaf area index (LAI) and normalized difference vegetation index (NDVI) for green-leaf vegetation from a subarctic study site, specifically to test whether relationships optimized for lower-latitude vegetation can be assumed to hold at higher latitudes. We focus attention particularly on dwarf-shrub vegetation, which has received little previous investigation. We have collected hyperspectral measurements of the optical properties (reflectance and absorptance) of single leaves from dwarf shrub and tree species common to northern European Russia, and have developed a simple physical model of the properties of assemblages ('leaf stacks') of these leaves. The model is shown to provide a satisfactory explanation of the effect of varying the number of leaves in a stack on its NDVI, and can be easily adapted to make simple measurements using relatively inexpensive equipment. Our results show that the LAI-NDVI relationship for a vegetation canopy will saturate (approach within 10% of its limiting value) when the LAI reaches a value of around 2 to 3. Values this low are not uncommon in subarctic vegetation. It is also shown that dwarf shrub vegetation may show lower NDVI than trees for the same LAI.

ARTICLE HISTORY

Received 4 February 2020
Accepted 24 May 2020

1. Introduction

At present, most of the maps describing structure, functions, productivity, the state and dynamics of vegetation are based on remote sensing imagery (Chen et al. 2015; Bartalev et al. 2015). The detail and scale of the maps vary depending on the image properties and the objectives of research. Spectral vegetation indices, such as the Normalized Difference Vegetation Index (NDVI; Tucker 1979) are among the most widely used tools to assess vegetation parameters with remote sensing data, in part because of the straightforwardness with which they can be calculated from suitable imagery and in part because of their close linkage to the physical properties of vegetation canopies. As a consequence, they find very widespread application in studies of vegetation distribution and its change over

CONTACT W. G. Rees  wgr2@cam.ac.uk  Scott Polar Research Institute, University of Cambridge, Cambridge CB2 1ER, UK

*Present address: Institute for Geosciences and Environmental Research, University of Grenoble, France

© 2020 Informa UK Limited, trading as Taylor & Francis Group

time (Pettorelli 2013). This is equally true of high northern latitudes as in other parts of the world. NDVI has been used to study the phenomenon of ‘greening of the Arctic’, and indeed ‘browning’ (Jia, Epstein, and Walker 2003; Phoenix and Bjerke 2016; Belonovskaya et al. 2016), including in Svalbard.

The NDVI is defined from the reflectance R in two spectral regions: visible red light (typically 0.6 to 0.7 μm), and the near-infrared (NIR: typically 0.7 to 1.0 μm). This exploits the absorption of red light by chlorophyll, and multiple scattering of infrared photons by the cellular structure of vascular plant tissue (Campbell 2008). The NDVI is defined as

$$\text{NDVI} = \frac{R_{\text{IR}} - R_{\text{red}}}{R_{\text{IR}} + R_{\text{red}}} \quad (1)$$

where ‘IR’ and ‘red’ denote near-infrared and red respectively. The definition can be applied at any spatial scale, from that of individual leaves to pixels or groups of pixels in a remotely sensed image, although it is most commonly used at the latter scale. It is meaningful at all scales, although the interpretation varies. At the scale of individual leaves, high photosynthetic activity generally corresponds to smaller reflectance values in the red and higher in the NIR, leading to higher NDVI. At the plot scale and coarser, the spatial distribution of leaves, and of vegetation units, is also relevant.

Other vegetation indices are also useful. Pettorelli (2013), following Bannari et al. (1995), lists 39 of them. Almost all of these indices combine reflectances in the red and near infrared bands, and of those that do so exclusively, many are monotonically related to the NDVI. Others incorporate other spectral bands. There are obvious limitations to the usefulness of spectral vegetation indices. In most cases, it is necessary to compare index-derived maps with field data at key sites, for calibration and validation. It is necessary to take into account natural phenological changes and seasonal changes of climatic parameters, which are particularly important for assessing plant productivity and other quantitative parameters. One other challenge in the use of vegetation indices is the varying density of the vegetation cover, which may include several canopy levels, and the differences in plant leaf structure. The use of vegetation indices is limited to the vegetation season.

The spatial distribution of leaves is partially captured by the concept of Leaf Area Index (LAI). Following the definition by Chen and Black (1992), this is defined by CEOS (the Committee on Earth Observation Satellites) as ‘one half of the total projected green leaf fractional area in the plant canopy within a given area’ (<http://database.eohandbook.com/measurements/measurements.aspx>). LAI is an important biophysical variable, for describing vegetation canopies and estimating productivity. It is generally increasing in the past decades, and in the subarctic regions the main driver is supposed to be climate change (Piao et al. 2020). The importance of the NDVI derives in large part from the fact that it is strongly correlated with LAI for a wide range of vegetation types, which suits it to mapping vegetation at a very general level (Zheng and Moskal 2009). This fact is also exploited in deriving estimates of LAI from remotely sensed data. The NDVI provides for very clear distinction between vegetation and non-vegetation objects in multispectral imagery that includes red and NIR bands. Typically, bare soils show NDVI values in the range 0.1 to 0.2, shrubs, grassland and senescing crops 0.2 to 0.5, while dense vegetation (including forests and crops at the peak of the growing season) reaches values of 0.6 to 0.9 (Pettorelli 2013). Boreal forests reach slightly lower values, of typically 0.6 to 0.8 (Parent and Verbyla 2010).

Shrubby understorey vegetation and dwarf shrub tundra can attain similar values of LAI (e.g. Lafleur and Humphreys 2018). Because it responds in such a general way to the presence of vascular plants, the NDVI is widely used to map vegetation distribution in a way that does not depend strongly on detailed knowledge of the vegetation composition. However, the relationship between LAI and NDVI is not unique. Health of vegetation affects the relationship strongly (although this is in part through changing the LAI itself), and this has often been exploited to map the impact of pollution (Rees 2012). Phenological variations can also be usefully exploited (Verbesselt et al. 2010) though they may also introduce undesirable uncertainty into the LAI-NDVI relationship (Wang et al. 2005), as can heterogeneity of vegetation type (Markon and Peterson 2002; Markon, Fleming, and Binnian 1995). However, if these confounding factors are controlled for (e.g. by considering only single species or at least vegetation types, unstressed and at peak greenness), the relationship between LAI and NDVI becomes fundamental.

Here, too, however, a difficulty may arise. The relationship is nonlinear and it saturates at sufficiently large values of NDVI (Turner et al. 1999; Gitelson 2004; Shabanov et al. 2005). The reason that saturation occurs is that at sufficiently high values of the LAI, the optical thickness of the canopy is large enough that no radiation penetrates it. The phenomenon thus depends on the optical properties of the leaves, and might also be expected to depend on the vegetation type. It also depends on the geometrical arrangement of the leaves within the canopy. This has been characterized by Chen's clumping index (Chen, Menges, and Leblanc 2005). Empirical studies based on temperate vegetation (Turner et al. 1999; Shabanov et al. 2005) suggest that the relationship saturates at values of LAI around 3 to 4. Typical LAI values in boreal forest may range up to 5 or 6 (Asner, Scurlock, and Hicke 2003), although values around 1 to 2 are more typical of tundra, so the possibility exists that the LAI-NDVI relationship for subarctic vegetation could saturate at inconveniently low values. Figure 1 shows the spatial distribution of LAI in part of the subarctic, estimated from MODIS (Moderate Resolution Imaging Spectrometer) imagery using an NDVI-dependent algorithm (Knyazikhin et al. 1999). Figure 2 shows a transect through this dataset, illustrating the fact that while dense boreal forest may have LAI values of 4 or more, values of 1 to 3 are more common at the northern margin of the forest and values around 1 are more representative of tundra areas. However, the accuracy of these values depends on the algorithm used to estimate LAI from satellite imagery, and the algorithm has been trained less extensively using data from the subarctic region than from other regions (Knyazikhin et al. 1999). More recently developed algorithms show in general similar values (Yang et al. 2006).

The aim of this paper is to investigate the relationship between LAI and NDVI for subarctic deciduous vegetation, using optical measurements of the leaves of a number of selected subarctic plant species. Unlike almost all other studies of NDVI for subarctic vegetation, the present investigation is based on optics at the finest (leaf-level) spatial scales. We develop a simple model of leaf optics that can be easily inverted to derive essential optical parameters from measurements that can be made in the field with relatively inexpensive equipment.

2. Modelling the dependence of NDVI on the properties of the leaf canopy

A number of more or less rigorous approaches to radiative transfer theory in a vegetation canopy have been developed in recent years (Shabanov et al. 2000; Shabanov and Gastellu-

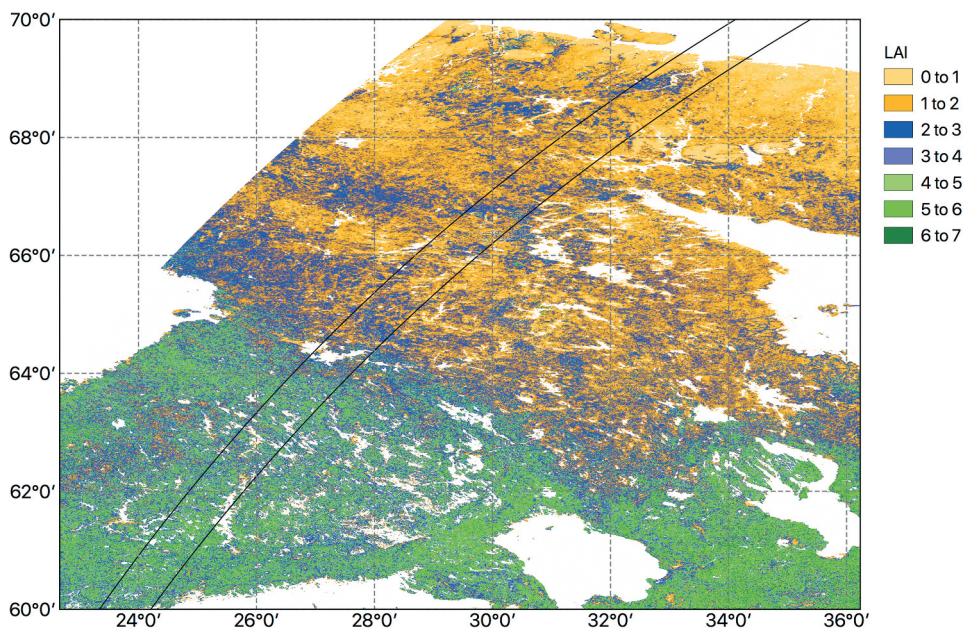


Figure 1. Annual maximum LAI values in northern Fennoscandia and the Kola Peninsula in 2019, calculated from MODIS MCD15A2 H 8 day composites (tile h19v02, shown in part). The latitudinal variation along the transect defined by the two lines is shown in Figure 2. Projection: Geographical (Plate Carrée), WGS84 datum. Pixel area 460 m × 460 m. Data downloaded from <https://lpdaac.usgs.gov/tools/data-pool/on> 16.01.2020 and processed using the freely available software Multispec (<https://engineering.purdue.edu/~biehl/MultiSpec/>), ImageJ (<https://imagej.nih.gov/ij/>) and QGIS (<https://www.qgis.org/en/site/>).

Etchegorry 2018). Our approach is simpler. We model a vegetation canopy straightforwardly as an assemblage of horizontally oriented leaves. If the LAI of this canopy is denoted by L , the spatial average of the number of leaves intercepted by a vertical path through the canopy is also given by L . However, the actual number of intercepted leaves n is likely to vary from one location to another with probability $p(n)$. The degree of clumping of the leaves is described by this probability distribution. Modelling the dependence of canopy reflectance (and hence of NDVI) on the value of L thus depends on considering the reflectance of a stack of n leaves as a function of n , as well as on the form of $p(n)$.

2.1. Relationship between n and L

We consider three cases. First, if the horizontal distribution of leaves is uniform, n can take either a value of

$$n_1 = \lfloor L \rfloor \quad (2)$$

with a probability

$$p(n_1) = \lfloor L \rfloor - L + 1 \quad (3)$$

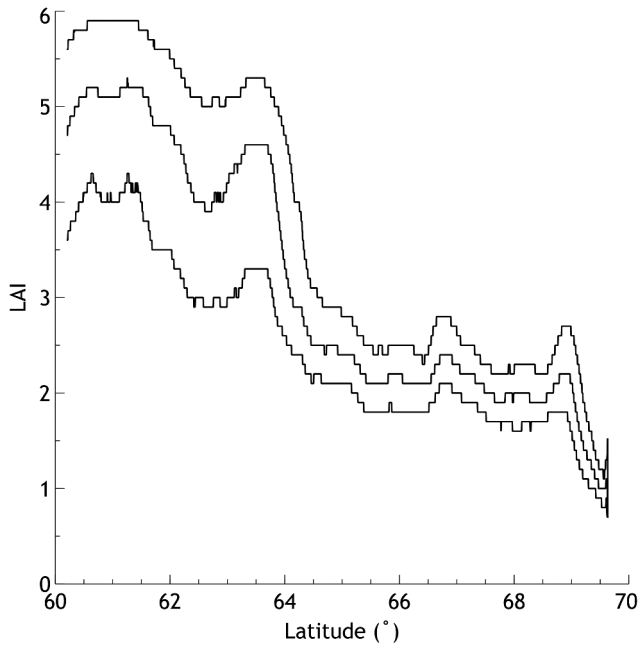


Figure 2. Median, lower and upper quartile LAI for 100×100 pixel ($46 \text{ km} \times 46 \text{ km}$) regions along the transect defined in Figure 1.

or a value of

$$n_2 = n_1 + 1 \quad (4)$$

with a probability

$$p(n_2) = L - \lfloor L \rfloor \quad (5)$$

(The symbol $\lfloor \cdot \rfloor$ denotes the floor, or largest integer not exceeding, function.) This represents the least clumped arrangement of leaves. Second, we consider the case where leaves are placed at random, so that n follows a Poisson distribution:

$$p(n) = \frac{L^n \exp(-L)}{n!} \quad (6)$$

Finally, we consider an example of extreme clumping. In this case, n can take either a value of n_{clump} , with a probability

$$p(n_{\text{clump}}) = \frac{L}{n_{\text{clump}}} \quad (7)$$

or a value of zero, with a probability

$$p(0) = 1 - p(n_{\text{clump}}) \quad (8)$$

The value of n_{clump} is assumed large enough to ensure that the relationship between LAI and reflectance saturates, i.e. that a further increase in n would not further increase the reflectance.

2.2. Relationship between stack reflectance, NDVI and n

In general, we denote the reflectance of a stack of n leaves at wavelength λ by $R(n, \lambda)$ so that Equation (1) can be written as

$$\text{NDVI}(n) = \frac{R(n, \lambda_{\text{IR}}) - R(n, \lambda_{\text{red}})}{R(n, \lambda_{\text{IR}}) + R(n, \lambda_{\text{red}})} \quad (9)$$

to represent the dependence of NDVI on the number of leaves, n , in a stack. The relationship between the optical properties of a single leaf and those of a stack of n leaves is derived by developing a simple two-stream model in which radiation can propagate only normal to the leaves. We suppose that the optical properties of a single leaf can be described by a wavelength-dependent reflection coefficient $\rho(\lambda)$ and a transmission coefficient $\tau(\lambda)$. We ignore the difference between the reflectances of upper and lower surfaces of a leaf (Carlson and Yarger 1971). The absorption coefficient $\alpha(\lambda)$ is thus given by

$$\alpha(\lambda) = 1 - \rho(\lambda) - \tau(\lambda) \quad (10)$$

In this case it is straightforward to show the recursive relationship

$$R(n, \lambda) = \rho(\lambda) + \frac{\tau^2(\lambda)R(n-1, \lambda)}{1 - \rho(\lambda)R(n-1, \lambda)} \quad (11)$$

where

$$R(0, \lambda) = R_g(\lambda) \quad (12)$$

is the reflectance of the ground beneath the canopy. In the limiting case of an infinite stack of leaves, (11) tends to a value of

$$R(\infty, \lambda) = \frac{1 + \rho^2(\lambda) - \tau^2(\lambda) - \sqrt{(1 + \rho^2(\lambda) - \tau^2(\lambda))^2 - 4\rho^2(\lambda)}}{2\rho(\lambda)} \quad (13)$$

We can use this simple model to calculate the number $n_{\text{max}}(\lambda)$ of leaves that give a stack reflectance that is sufficiently close to that of an infinite stack of leaves. Specifically, we define $n_{\text{max}}(\lambda)$ as the smallest integer m that satisfies

$$R(m, \lambda) \geq kR(\infty, \lambda) \quad (14)$$

where k , which measures the extent of convergence to the reflectance of an infinite stack, is taken to be either 0.90 or 0.99. If $n_{\text{max}}(\lambda) \approx 1$, the optical properties of a single leaf at that wavelength are similar to those of a stack of many leaves, while if $n_{\text{max}}(\lambda) \gg 1$, they will be very different. In general, we would not expect the values of $n_{\text{max}}(\lambda)$ to be the same at different wavelengths so the reflectance-LAI dependence would saturate at different values of LAI for different wavelengths. In calculating a vegetation index such as the NDVI, it would then be the wavelength with the largest value of $n_{\text{max}}(\lambda)$ that would determine the LAI at which the NDVI value would saturate. Since the absorption coefficient $\alpha(\lambda)$ of leaves is much larger in the visible than the near infrared part of the spectrum, it is the latter that has the dominant effect on saturation of the relationship.

3. Materials and methods

We collected *in vivo* hyperspectral reflectance data, to characterize their reflectance spectra across the visible and near-infrared regions, from a wide range of leaves characteristic of subarctic ecosystems in northern European Russia. Fieldwork was carried out in June–July, i.e. close to the peak of greenness, in 2012, 2013 and 2014. The location of the fieldwork was in the centre of the Kola Peninsula, in and around the Khibiny and Lovozero mountains (Figure 3), chosen to include mountain birch forests and mountain tundra areas. Leaf samples were selected from amongst dwarf shrub and tree species found typically in this region. Measurements were performed using the hyperspectral field-portable spectroradiometer ‘FieldSpec 3 Hi-Res’ (ASD Inc.), designed to measure absolute radiance values and reflectance, with a spatial resolution of 3 nm in the region 350 to 1000 nm and 10 nm in the region 1000 to 2500 nm. We made contact measurements of leaves using the ASD leaf clip (<https://www.asdi.com/products-and-services/accessories/leaf-clip>) which allowed the reflectance properties to be measured from a leaf, or more than one leaf, held securely in a frame against a non-reflective background. We measured the properties of ‘leaf stacks’ (Lillesaeter 1982; Martin and Aber 1990; Jacquemoud et al. 1996; Dawson, Curran, and Plummer 1998; Blackburn 1999; Neuwirthová, Lhotáková, and Albrechtová 2017), stacks of various numbers of leaves representing a range of tree and dwarf shrub species collected from the study area. The reflectance data measured using the leaf clip (25 readings per sample) were spectrally averaged to the ranges 600 to 700 nm, to represent the red visible part of the spectrum, and 700 to 1300 nm, to represent the near-infrared part of the spectrum. Parameter-fitting of the model described by Equations (11) and (12) was performed in GNU Octave. In addition an ASD Inc. RTS-3ZC integrating sphere was used to

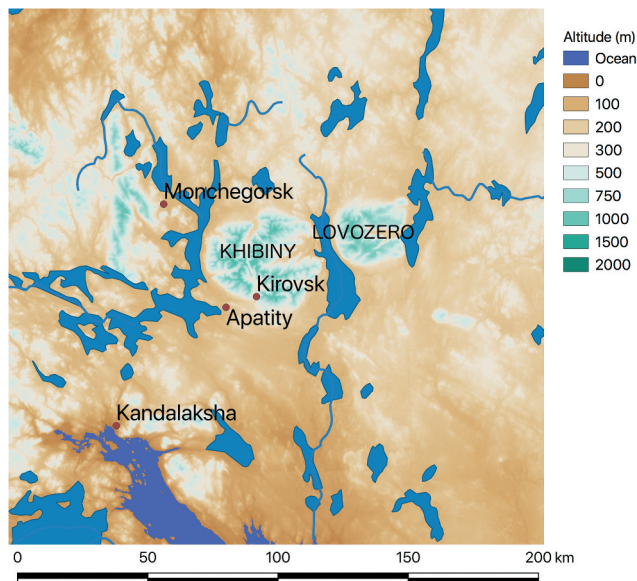


Figure 3. Location of the Khibiny and Lovozero Mountains in the central Kola Peninsula, Russia. Map prepared using QGIS from data obtained from Natural Earth (www.naturalearthdata.com) and USGS DTED (https://topotools.cr.usgs.gov/gmted_viewer/viewer.htm).

make direct measurements of the spectral reflectance and transmittance of a single leaf of *Betula pubescens*. This is a particularly important species in its own right, and the spectrally detailed direct measurements also help us to understand the implications of [section 2](#) for vegetation indices in general.

4. Results

Reflectance and transmittance spectra of *Betula pubescens*, determined using the integrating sphere, are shown in [Figure 4](#). In view of the widespread importance of this species in subarctic vegetation, we also provide the data in digital form (<https://doi.org/10.17863/CAM.52922>). The corresponding value of n_{\max} , calculated from [Equations \(9\)–\(12\)](#) assuming $R_g = 0$, is shown in [Figure 5](#).

The results for *Betula pubescens*, though perhaps unsurprising in view of the published literature on optical properties of leaves in general, aid in the interpretation of the results from other species for which we were unable to collect such detailed measurements. [Figure 6](#) shows, as a typical example, one of the twelve sets of leaf-stack measurements collected using the leaf clip. This shows clear evidence of increasing reflectance as the number n of leaves in the stack increases, as indicated by [Equation \(10\)](#), markedly so in the near infrared region but also discernibly, though with some fluctuations, in the visible region of the spectrum. This behaviour is, unsurprisingly, similar to that reported by Neuwirthová, Lhotáková, and Albrechtová (2017).

Results of fitting [Equation \(10\)](#) to the leaf-stack measurements are summarized in [Table 1](#). [Figure 7](#) shows the measured visible and NIR reflectances, averaged over the wavelength ranges 600 to 700 and 700 to 1300 nm, as functions of the number n of leaves in the stack. The figure also shows the modelled values of reflectance using [Equation \(10\)](#) and the best-fitting values of ρ and τ . We note here that the equation gives a convincing fit to the data in

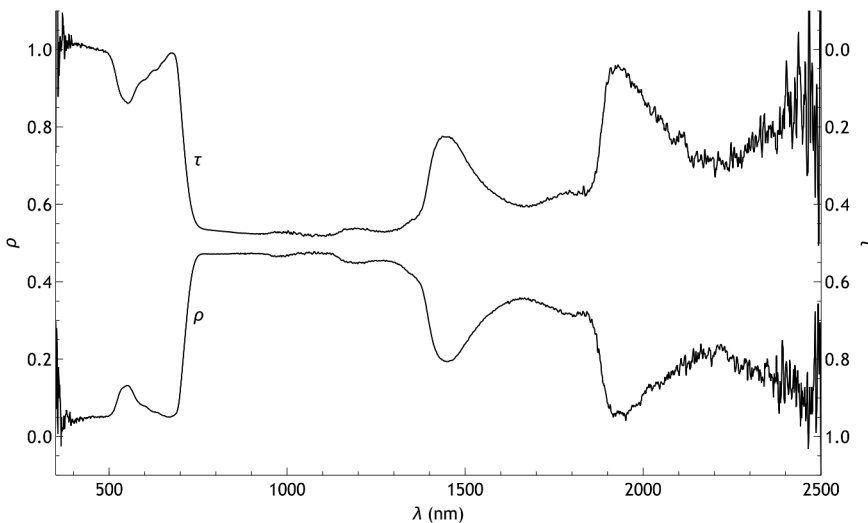


Figure 4. Reflectance ρ and transmittance τ of a single *Betula pubescens* leaf measured using an integrating sphere. The distance between the two lines corresponds to the absorbance a .

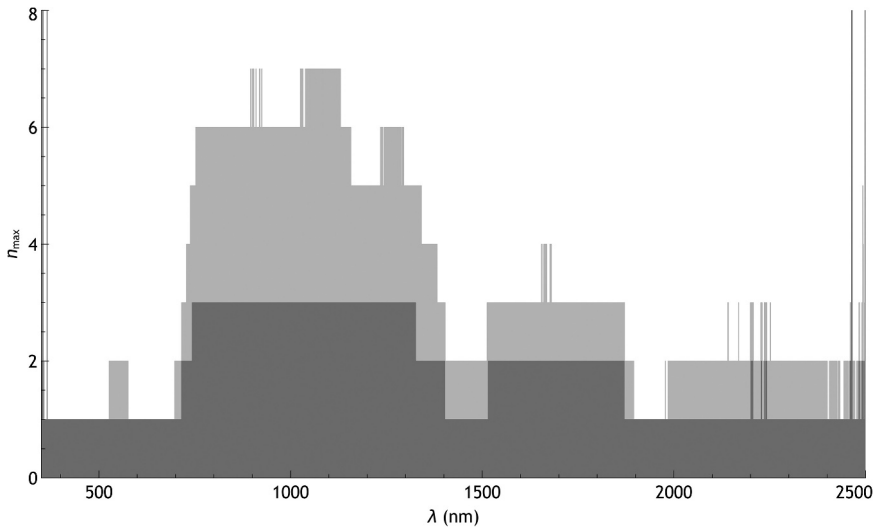


Figure 5. Calculated value of n_{\max} corresponding to Figure 4, for convergence factors $k = 0.90$ (dark grey) and 0.99 (light grey).

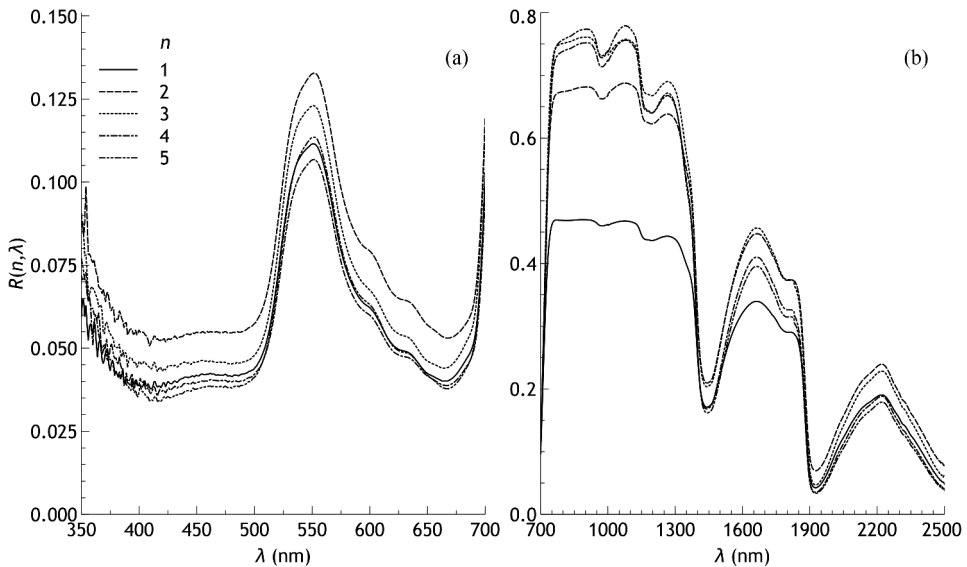


Figure 6. Spectral reflectance of a stack of n leaves of *Betula tortuosa*, for $n = 1$ to 5. (a): 350 to 700 nm; (b): 700 to 2500 nm.

most cases, and that where more than one set of measurements was available for a particular species the results were generally consistent.

Best-fitting values of ρ and τ from Table 1 were used to model the dependence of NDVI on LAI according to the three models developed in section 2. R_g was taken as 0.09 for red and 0.11 for infrared, based on our spectral reflectance measurements of bare ground. The results are presented in Figure 8, distinguished between tree and dwarf shrub species.

Table 1. Values of ρ and τ in the visible and NIR regions, derived by fitting Equations (8)–(11) to reflectance measurements made from leaf stacks. In each case the best-fitting, minimum and maximum value of each parameter is shown.

Species	Waveband (nm)											
	600 to 700						700 to 1300					
	ρ			τ			ρ			τ		
	Best	Min	Max	Best	Min	Max	Best	Min	Max	Best	Min	Max
<i>Alnus</i> sp.	0.06	0.06	0.07	0.32	0.24	0.94	0.46	0.45	0.46	0.52	0.52	0.54
<i>Betula nana</i>	0.05	0.04	0.06	0.06	0.00	0.34	0.46	0.46	0.46	0.52	0.52	0.52
<i>Betula tortuosa</i>	0.05	0.05	0.06	0.27	0.00	0.42	0.48	0.46	0.49	0.48	0.46	0.50
<i>Betula tortuosa</i>	0.05	0.04	0.05	0.17	0.00	0.26	0.46	0.46	0.46	0.50	0.50	0.50
<i>Betula tortuosa</i>	0.05	0.04	0.05	0.00	0.00	0.28	0.48	0.47	0.48	0.48	0.47	0.48
<i>Salix lanata</i>	0.08	0.07	0.09	0.09	0.00	0.32	0.47	0.47	0.48	0.50	0.49	0.50
<i>Salix</i> sp.	0.08	0.08	0.09	0.21	0.00	0.34	0.44	0.44	0.45	0.54	0.53	0.55
<i>Salix</i> sp.	0.05	0.05	0.06	0.43	0.39	0.46	0.43	0.43	0.44	0.56	0.55	0.56
<i>Sorbus</i> sp.	0.06	0.05	0.06	0.00	0.00	0.24	0.47	0.44	0.49	0.50	0.46	0.50
<i>Vaccinium myrtillus</i>	0.07	0.06	0.07	0.07	0.00	0.26	0.33	0.32	0.33	0.67	0.66	0.67
<i>Vaccinium myrtillus</i>	0.06	0.06	0.07	0.00	0.00	0.24	0.47	0.44	0.50	0.41	0.35	0.45
<i>Vaccinium uliginosum</i>	0.05	0.05	0.06	0.40	0.33	0.45	0.43	0.42	0.43	0.55	0.55	0.56

5. Discussion

Indirect measurements of the optical properties, measured using stacks of leaves of various forest and tundra species, can be simply but convincingly modelled using the two-stream radiative transfer model (Figure 7). This has the advantage of simplicity and it could easily be adapted to measurements taken in the field using a relatively inexpensive USB spectrometer. Our measurements are consistent with visible-wavelength (600 to 700 nm) reflectances in the range 0.05 to 0.08 (Table 1). Visible-wavelength transmittances are rather poorly constrained by this method, though most of the best-fitting values are below 0.2 and in only one case out of 12 was the maximum likely value of the transmittance greater than 0.40 (Table 1). Direct measurement of the optical properties of a leaf of *Betula pubescens*, using an integrating sphere, shows that it has a reflectance and a transmittance both around 0.1 in the visible region (Figure 4), with a minimum absorptance around 0.8 occurring at about 550 nm, broadly consistent with both the general features expected from green leaves (Breece and Holmes 1971) and with the value deduced from our model-fitting.

Indirect (leaf-stack) measurements of the NIR (700 to 1300 nm) characteristics of the leaf samples were also for the most part convincingly modelled by the two-stream model (Figure 7), with reflectances typically around 0.4 and transmittances around 0.55 (Table 1). These are again broadly comparable with the values (around 0.45 and 0.45 respectively) obtained by direct measurement from a leaf of *Betula pubescens* (Figure 4). The apparently anomalous behaviour of one of the samples of *Vaccinium myrtillus* (Figure 7) is possibly due to drying out of the leaf samples in the leaf clip during an unusually prolonged series of measurements.

Even with the lowest observed value of the best-fitting absorptance the two-stream radiative transfer model implies that the dependence of stack reflectance on n will saturate (in the stricter sense with $k = 0.99$) at $n \approx 3$. For most of the observed values of the optical properties, including those derived directly using the integrating sphere, the saturation occurs at an even lower value of n . In the 700 to 1300 nm NIR region, the fitted reflectances lie in the range 0.33 to 0.48, transmittances in the range 0.41 to 0.67 and

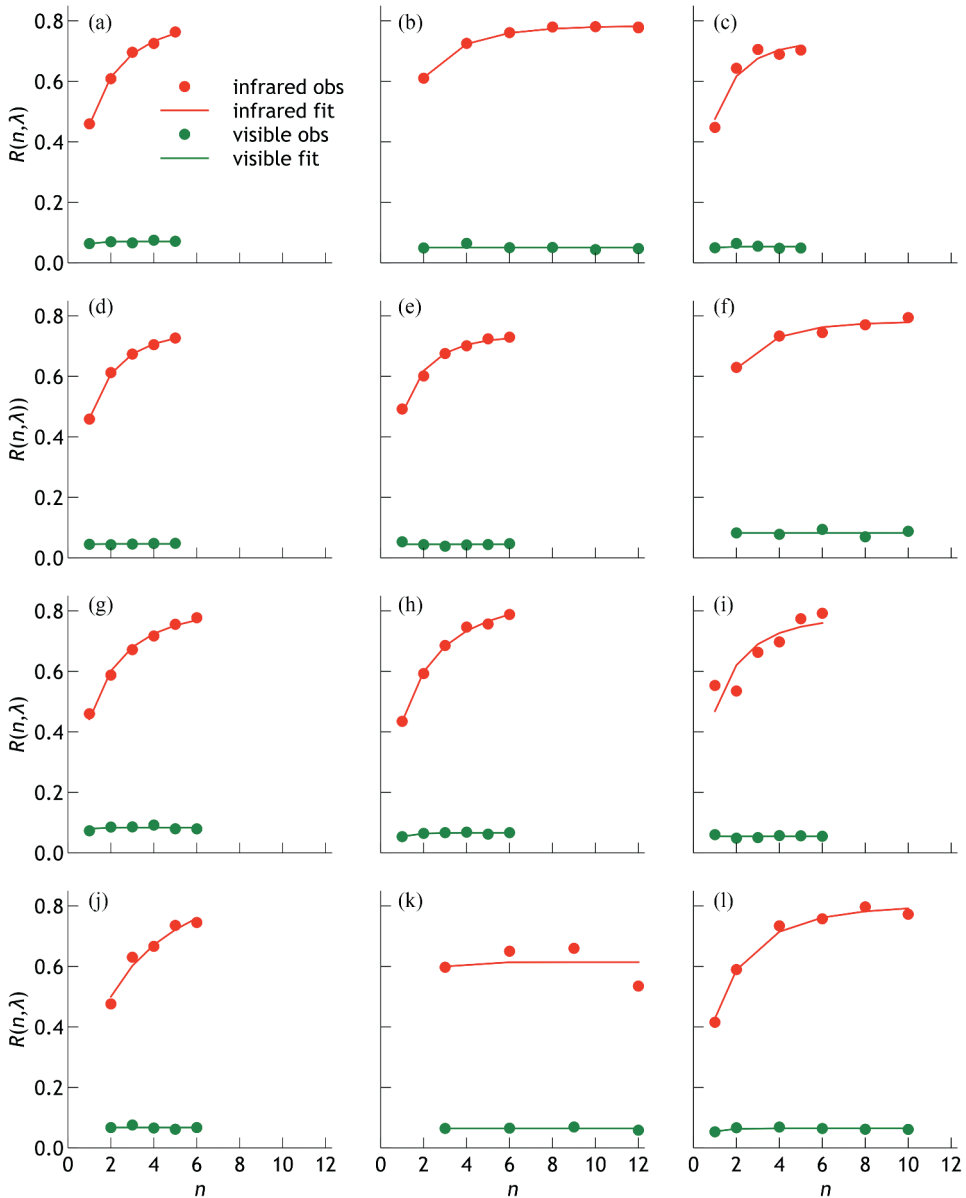


Figure 7. Observed (dots) and fitted (lines) reflectances R of leaf stacks as a function of the number of leaves n in the stack. Green = visible, red = NIR. (a) *Alnus sp.*, (b) *Betula nana*, (c) *Betula tortuosa*, (d) *Betula tortuosa*, (e) *Betula tortuosa*, (f) *Salix lanata*, (g) *Salix sp.*, (h) *Salix sp.*, (i) *Sorbus sp.*, (j) *Vaccinium myrtillus*, (k) *Vaccinium myrtillus*, (l) *Vaccinium uliginosum*.

absorptances in the range 0.01 to 0.12. Both the reflectance and the transmittance are in general well constrained by the leaf-stack method in this part of the spectrum. Modelling using the two-stream radiative transfer model implies that the dependence of stack reflectance on n will not saturate until n reaches a value of at least 4, with most measurements implying a value of n_{\max} in the range 6 to 10. Using the looser definition

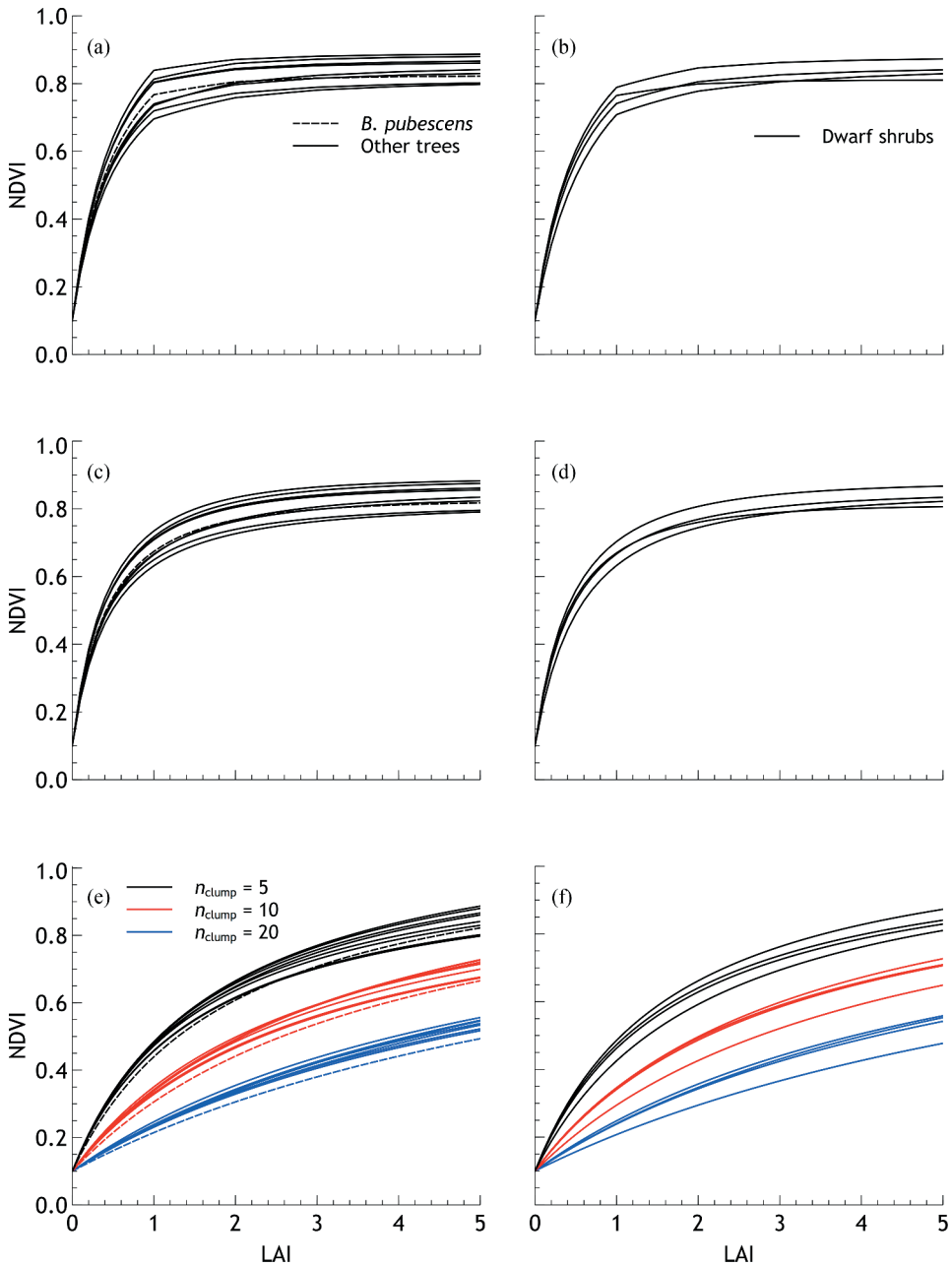


Figure 8. Dependence of NDVI on LAI for the species measured in this paper. Top row (a and b): uniform model; middle row (c and d): Poisson model; bottom row (e and f): clumped model with values of $n_{clump} = 5$ (black), 10 (red) and 20 (blue). Left column (a, c and e): tree species (*Betula pubescens* shown dashed); right column (b, d and f): dwarf shrub species.

of saturation $k = 0.90$, the limiting value of n would be correspondingly reduced, to around 2 to 3.

The measurements presented here are derived from single leaves. They can be cautiously extrapolated to dependence of NDVI on LAI at plot and field scale using [Equations \(2\)–\(8\)](#). In

all of the spatial models of leaf distribution described earlier (uniform, Poisson and highly clumped) it is necessary to consider the case $n = 0$, i.e. when no leaves at all intercept the path of a ray of light through the vegetation canopy. This is particularly important in the highly clumped model, where most of the canopy consists of holes. Figure 9 shows the NDVI-LAI relationship assumed by the MODIS algorithm for the two most relevant biomes, namely broadleaf and needle-leaf forests (Knyazikhin et al. 1999, Figures 2–12(c), adapted). The similarity of Figure 8(c) (NDVI – LAI relationship extrapolated from our results to tree canopies assuming Poisson distributed leaves) to Figure 9 suggests that the Poisson model is realistic, and that the assumptions of the MODIS LAI algorithm are reasonable for vegetation canopies composed of leaves such as those investigated here. The similarity of Figure 8(c,d), which follows from the similar optical characteristics of tree leaves and those of dwarf shrubs, further suggests that the algorithm is also valid for dwarf shrub tundra. Comparison of the left side (a, c and e) to the right side (b, d and f) of Figure 8 implies that, if differences in optical properties alone are taken into account (i.e. there are no differences in the geometrical arrangements of the leaves), the NDVI of a dwarf shrub species will be less than that of a tree species having the same LAI, or equivalently, that the LAI of a dwarf shrub would be overestimated from its NDVI if the relationship were calibrated from tree species. This is consistent with the fact that woody vegetation saturates at a higher value of NDVI than herbaceous vegetation (Shabanov et al. 2005).

Two important conclusions can be drawn from these results. The first concerns the extent to which the measurement of the reflectance of a single leaf represents the properties of an optically thick canopy. Figure 6 shows that, while this is largely true in the visible part of the spectrum, leaf transparency means that it far from true in the 700 to 1300 nm region. Reflectance measurements of a single leaf will be significantly affected, in

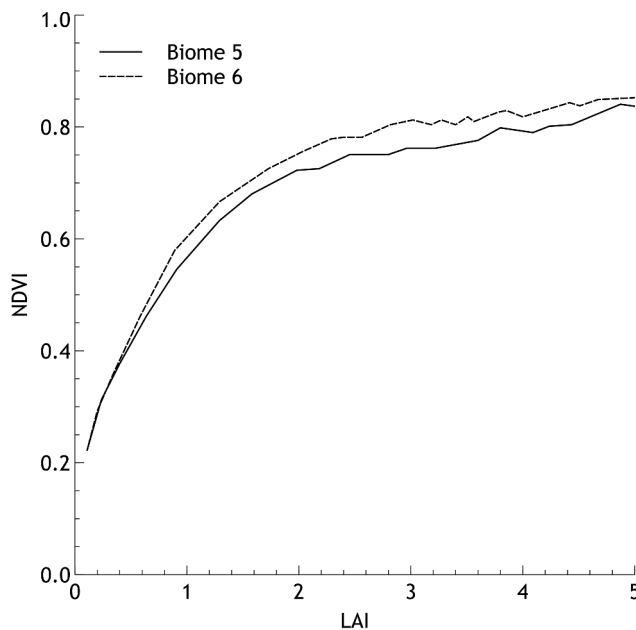


Figure 9. Best estimate of NDVI from LAI for Biome 5 (broadleaf forest) and Biome 6 (needleleaf forest) according to the MODIS algorithm (Knyazikhin et al. 1999).

this part of the spectrum, by whatever lies behind the leaf. This point has also been made by Neuwirthová, Lhotáková, and Albrechtová (2017). Secondly, we can deduce that a vegetation index derived using reflectance measurements in this part of the IR spectrum will not saturate (in the sense of approaching to within 1% of the limiting value) until the LAI reaches a value of typically around 6, which is higher – though not dramatically so – than the maximum values reported for subarctic vegetation. However, if the definition of saturation is relaxed to mean that the reflectance is within 10% of the limiting value, the vegetation index will saturate at LAI values around 2 to 3, within the range of values encountered in subarctic vegetation.

We have measured the optical properties of a range of leaves corresponding to different types of subarctic vegetation, using both direct measurement in an integrating sphere and also simulations of vegetation canopies consisting of stacks of leaves. The leaf-stack method is a particularly simple way of measuring the optical properties of leaves, since it dispenses with the need for an integrating sphere, and thus increases the opportunities for making such measurements. A simple two-stream radiative transfer model satisfactorily explains the behaviour of leaf stacks as a function of the number of leaves. The results of the two methods are broadly consistent, and show that the transparency of leaves in the near infrared region, especially from around 700 to 1300 nm, is far from negligible. This implies that a reflectance measurement made for a single leaf is not representative of that of an optically thick canopy – a stack of around 10 leaves would be needed to comfortably assure this. It also implies that the dependence on leaf area index of vegetation indices that use this range of wavelengths does not saturate (in the sense of approaching to within 1% of its optically thick value) until the LAI reaches a value of around 6, which is higher than that normally encountered in subarctic vegetation canopies. However, the relationship between NDVI and LAI weakens considerably above LAI values as low as 1 or 2 (depending on the assumed distribution of leaves). These results are broadly consistent with the assumptions made in deriving estimates of LAI from MODIS imagery, and provide some reassurance that the MODIS algorithm is valid not just for boreal forest but also dwarf shrub dominated tundra. However, some differences are apparent between the tree species and dwarf shrub species investigated here, such that, for the same geometrical distribution of leaves and LAI, dwarf shrubs would exhibit a lower NDVI than trees.

Acknowledgements

WGR, OVT, EIG, and MVZ and have been supported by the The Russian-British project “Multiplatform remote sensing of the impact of climate change on northern forests of Russia” unded by the British Council (Institutional Links Programme Grant no. 352397111) and the Ministry of Science and Higher Education of the Russian Federation (project RFMEFI61618X0099). The FieldSpec Pro Hi-Res spectroradiometer was purchased under the Development Programme of M. V. Lomonosov Moscow State University. The SLAP project to create a spectral library was supported in 2014–2017 by the EU ‘Interact’ programme to support the research and education network of Arctic research stations (www.eu-interact.org).

Disclosure statement

The authors declare that they have no conflicts of interest in the research described in this paper.

Funding

This work was supported by the British Council [352397111]; Ministry of Science and Higher Education of the Russian Federation [RFMEFI61618X0099].

ORCID

W. G. Rees  <http://orcid.org/0000-0001-6020-1232>
 E. I. Golubeva  <http://orcid.org/0000-0001-9595-5974>
 O. V. Tutubalina  <http://orcid.org/0000-0001-8049-1724>
 M. V. Zimin  <http://orcid.org/0000-0003-4789-2192>
 A. A. Derkacheva  <http://orcid.org/0000-0002-7386-3814>

References

- Asner, G. P., J. M. O. Scurlock, and J. A. Hicke. 2003. "Global Synthesis of Leaf Area Index Observations: Implications for Ecological and Remote Sensing Studies." *Global Ecology and Biogeography* 12 (3): 191–205. doi:10.1046/j.1466-822X.2003.00026.x.
- Bannari, A., D. Morin, F. Bonn, and A. R. Huete. 1995. "A Review of Vegetation Indices." *Remote Sensing Reviews* 13 (1–2): 95–120. doi:10.1080/02757259509532298.
- Bartalev, S. A., V. A. Egorov, V. O. Zharko, E. A. Lupyan, D. E. Plotnikov, and S. A. Khvostikov. 2015. "Status and Prospects of Development of Satellite Mapping Methods for the Vegetation Cover of Russia Current State and Development Prospects of Satellite Mapping Methods of Russia's Vegetation Cover." *Modern Current Problems in Remote Sensing of the Earth from Space* 12 (5), (in Russian): 203–221.
- Belonovskaya, E. A., A. A. Tishkov, M. A. Weissfeld, P. M. Glazov, A. N. Krenke Jr, O. V. Morozova, I. V. Pokrovskaya, N. G. Tsarevskaya, and G. M. Tertitsky. 2016. "Greening" of the Russian Arctic and Current Trends in Changing Its Biota." *Proceedings of the Russian Academy of Sciences. Series Geographical* 3: 28–39. (In Russian).
- Blackburn, G. A. 1999. "Relationships between Spectral Reflectance and Pigment Concentrations in Stacks of Deciduous Broadleaves." *Remote Sensing of Environment* 70: 224–237. doi:10.1016/S0034-4257(99)00048-6.
- Breece, H. T., and R. A. Holmes. 1971. "Bidirectional Scattering Characteristics of Healthy Green Soybean and Corn Leaves in Vivo." *Applied Optics* 10 (1): 119–127. doi:10.1364/AO.10.000119.
- Campbell, J. B. 2008. *Introduction to Remote Sensing*. 4th ed. New York: Guilford Press.
- Carlson, R. E., and D. N. Yarger. 1971. "An Evaluation of Two Methods for Obtaining Leaf Transmissivity from Leaf Reflectivity Measurements." *Agronomy Journal* 63: 78–81. doi:10.2134/agronj1971.00021962006300010024x.
- Chen, J. M., and T. A. Black. 1992. "Defining Leaf Area Index for Non-Flat Leaves." *Plant, Cell & Environment* 15 (4): 421–429. doi:10.1111/j.1365-3040.1992.tb00992.x.
- Chen, J. M., C. H. Menges, and S. G. Leblanc. 2005. "Global Mapping of Foliage Clumping Index Using Multi-Angular Satellite Data." *Remote Sensing of Environment* 97 (4): 447–457. doi:10.1016/j.rse.2005.05.003.
- Chen, J., J. Chen, A. Liao, X. Cao, L. Chen, X. Chen, C. He, et al. 2015. "Global Land Cover Mapping at 30m Resolution: A POK-Based Operational Approach." *ISPRS Journal of Photogrammetry and Remote Sensing, Global Land Cover Mapping and Monitoring* 103 (May): 7–27. doi:10.1016/j.isprsjprs.2014.09.002.
- Dawson, T. P., P. J. Curran, and S. E. Plummer. 1998. "LIBERTY - Modeling the Effects of Leaf Biochemical Concentration on Reflectance Spectra." *Remote Sensing of Environment* 65: 50–60. doi:10.1016/S0034-4257(98)00007-8.
- Gitelson, A. A. 2004. "Wide Dynamic Range Vegetation Index for Remote Quantification of Biophysical Characteristics of Vegetation." *Journal of Plant Physiology* 161 (2): 165–173. doi:10.1078/0176-1617-01176.

- Jacquemoud, S., S. L. Ustin, J. Verdebout, G. Schmuck, G. Andreoli, and B. Hosgood. 1996. "Estimating Leaf Biochemistry Using the PROSPECT Leaf Optical Properties Model." *Remote Sensing of Environment* 56: 194–202. doi:10.1016/0034-4257(95)00238-3.
- Jia, G. J., H. E. Epstein, and D. A. Walker. 2003. "Greening of Arctic Alaska, 1981–2001." *Geophysical Research Letters* 30 (20). doi:10.1029/2003GL018268.
- Knyazikhin, Y., J. Glassy, J. L. Privette, Y. Tian, A. Lotsch, Y. Zhang, Y. Wang, et al. 1999. "MODIS Leaf Area Index (LAI) and Fraction of Photosynthetically Active Radiation Absorbed by Vegetation (FPAR) Product (MOD15) Algorithm Theoretical Basis Document." <http://eosps0.gsfc.nasa.gov/atbd/modistables.html>
- Lafleur, P. M., and E. R. Humphreys. 2018. "Tundra Shrub Effects on Growing Season Energy and Carbon Dioxide Exchange." *Environmental Research Letters* 13 (5): 061001. doi:10.1088/1748-9326/aab863.
- Lillesaeter, O. 1982. "Spectral Reflectance of Partly Transmitting Leaves: Laboratory Measurements and Mathematical Modeling." *Remote Sensing of Environment* 12: 247–254. doi:10.1016/0034-4257(82)90057-8.
- Markon, C. J., M. D. Fleming, and E. F. Binnian. 1995. "Characteristics of Vegetation Phenology over the Alaskan Landscape Using AVHRR Time-Series Data." *Polar Record* 31 (177): 179–190. doi:10.1017/S0032247400013681.
- Markon, C. J., and K. M. Peterson. 2002. "The Utility of Estimating Net Primary Productivity over Alaska Using Baseline AVHRR Data." *International Journal of Remote Sensing* 23 (21): 4571–4596. doi:10.1080/01431160110113926.
- Martin, M. E., and J. D. Aber. 1990. "Effects of Moisture Content and Chemical Composition on the near Infrared Spectra of Forest Foliage." *Imaging Spectroscopy of the Terrestrial Environment* 1298: 171–177.
- Neuwirthová, E., Z. Lhotáková, and J. Albrechtová. 2017. "The Effect of Leaf Stacking on Leaf Reflectance and Vegetation Indices Measured by Contact Probe during the Season." *Sensors* 17: 1202. doi:10.3390/s17061202.
- Parent, M. B., and D. Verbyla. 2010. "The Browning of Alaska's Boreal Forest." *Remote Sensing* 2 (12): 2729–2747. doi:10.3390/rs2122729.
- Pettorelli, N. 2013. *The Normalized Difference Vegetation Index*. Oxford, New York: Oxford University Press.
- Phoenix, G. K., and J. W. Bjerke. 2016. "Arctic Browning: Extreme Events and Trends Reversing Arctic Greening." *Global Change Biology* 22 (9): 2960–2962. doi:10.1111/gcb.13261.
- Piao, S., X. Wang, T. Park, C. Chen, X. Lian, Y. He, J. W. Bjerke, et al. 2020. "Characteristics, Drivers and Feedbacks of Global Greening." *Nature Reviews Earth & Environment* 1:14–27. doi:10.1038/s43017-019-0001-x.
- Rees, W. G. 2012. "Automated Spaceborne Detection of Degraded Vegetation around Monchegorsk, Kola Peninsula, Russia." *Polar Record* 48: 107–112. doi:10.1017/S0032247411000337.
- Shabanov, N., and J.-P. Gastellu-Etchegorry. 2018. "The Stochastic Beer–Lambert–Bouguer Law for Discontinuous Vegetation Canopies." *Journal of Quantitative Spectroscopy and Radiative Transfer* 214 (July): 18–32. doi:10.1016/j.jqsrt.2018.04.021.
- Shabanov, N. V., Y. Knyazikhin, F. Baret, and R. B. Myneni. 2000. "Stochastic Modeling of Radiation Regime in Discontinuous Vegetation Canopies." *Remote Sensing of Environment* 74 (1): 125–144. doi:10.1016/S0034-4257(00)00128-0.
- Shabanov, N. V., D. Huang, W. Yang, B. Tan, Y. Knyazikhin, R. B. Myneni, D. E. Ahl, et al. 2005. "Analysis and Optimization of the MODIS Leaf Area Index Algorithm Retrievals over Broadleaf Forests." *IEEE Transactions on Geoscience and Remote Sensing* 43 (8): 1855–1865. doi:10.1109/TGRS.2005.852477.
- Tucker, C. J. 1979. "Red and Photographic Infrared Linear Combinations for Monitoring Vegetation." *Remote Sensing of Environment* 8 (2): 127–150. doi:10.1016/0034-4257(79)90013-0.
- Turner, D. P., W. B. Cohen, R. E. Kennedy, K. S. Fassnacht, and J. M. Briggs. 1999. "Relationships between Leaf Area Index and Landsat TM Spectral Vegetation Indices across Three Temperate Zone Sites." *Remote Sensing of Environment* 70 (1): 52–68. doi:10.1016/S0034-4257(99)00057-7.

- Verbesselt, J., R. Hyndman, A. Zeileis, and D. Culvenor. 2010. "Phenological Change Detection while Accounting for Abrupt and Gradual Trends in Satellite Image Time Series." *Remote Sensing of Environment* 114 (12): 2970–2980. doi:[10.1016/j.rse.2010.08.003](https://doi.org/10.1016/j.rse.2010.08.003).
- Wang, Q., A. Samuel, J. Tenhunen, and A. Granier. 2005. "On the Relationship of NDVI with Leaf Area Index in a Deciduous Forest Site." *Remote Sensing of Environment* 94 (2): 244–255. doi:[10.1016/j.rse.2004.10.006](https://doi.org/10.1016/j.rse.2004.10.006).
- Yang, W., N. V. Shabanov, D. Huang, W. Wang, R. E. Dickinson, R. R. Nemani, Y. Knyazikhin, and R. B. Myneni. 2006. "Analysis of Leaf Area Index Products from Combination of MODIS Terra and Aqua Data." *Remote Sensing of Environment* 104 (3): 297–312. doi:[10.1016/j.rse.2006.04.016](https://doi.org/10.1016/j.rse.2006.04.016).
- Zheng, G., and L. M. Moskal. 2009. "Retrieving Leaf Area Index (LAI) Using Remote Sensing." *Sensors* 9: 2719–2745. doi:[10.3390/s90402719](https://doi.org/10.3390/s90402719).